ANALYSIS OF THE INTERACTIONS OF MIGRATING MACROPHAGES

José Alonso Solís-Lemus[1], Brian Stramer[2], Greg Slabaugh[1,3], and Constantino Carlos Reyes-Aldasoro[1]

[1] School of Mathematics, Computer Science and Engineering, City, University of London, UK
[2] Randall Division of Cell & Molecular Biophysics, King's College London, UK
[3] Huawei Technologies Research & Development, London, UK

Abstract. Understanding the migrating patterns of cells in the immune system is of great importance; especially the changes of direction and its cause. For macrophages and other immune cells, excessive migration could be related to autoimmune diseases and cancer. In this work, an algorithm to analyse the change in direction of cells before and after they interact with another cell is proposed. The main objective is to provide insights into the notion that interactions between cell structures appear to anticipate migration. Such interactions are determined when the cells overlap and form *clumps* of two or more cells. The algorithm integrates a segmentation technique capable of detecting overlapping cells and a tracking framework into a tool for the analysis of the trajectories of cells before and after they overlap. The preliminary results show promise into the analysis and the hypothesis proposed, and it lays the ground work for further developments.

Keywords: Segmentation, Cell Tracking, Track analysis, Macrophages

1 INTRODUCTION

The immune system is one of the biological systems where cell migration performs a key task [1,2]. Macrophages are cells of the immune system that filter foreign particles when settled in lymphoid tissues and the liver [1]. In homeostasis, or the tendency to an equilibrium of physiological processes, the role of macrophages range from tissue repair through to immune responses to pathogens [3]. However, excessive migration can be related to autoimmune diseases and cancer [4]. The model organism *Drosophila melanogaster* has led to clues of how these cells integrate environmental cues into migration patterns [2]; interactions amongst the cells' structures appear to anticipate the direction of migration [5] as the observation of cells in humans is complicated.

Cell segmentation, the correct identification of a cell from other cells and background, and tracking, linking detected objects in one time frame to the objects in the following time frames, has been widely studied [6,7,8,9]. Cellular events, such as the interaction between cells, are also of importance. In [6],

several tracking algorithms were evaluated with a series migratory cells with very different conditions, not only in their ability to track detected objects, but also to identify cellular events, like mitosis. In [10], the analysis of the trajectories of crustaceans observed in microfluidic settings produced by the tracking algorithm was used to provide insights on an external state of the segmented objects, i.e. the health of the environment. In a similar setting as the work here presented, the tracking of fluorescently labelled macrophages in single frames has been done [11], showcasing the complex interactions the cells that manifest as overlapping (defined as *clumps*) and segmentations.

In this work, an algorithm to analyse the movement of fluorescently labelled macrophages is proposed. Particular emphasis is placed in the analysis of the cells' trajectories and the interaction between cells. The algorithm integrates the segmentation algorithm described in [11] into the software framework PhagoSight [12], and utilises the overlapped clumps as points of interaction between the cells. The main hypothesis of this work is that the direction of a given cell will change noticeably before and after an interaction with another cell (Figure 1).

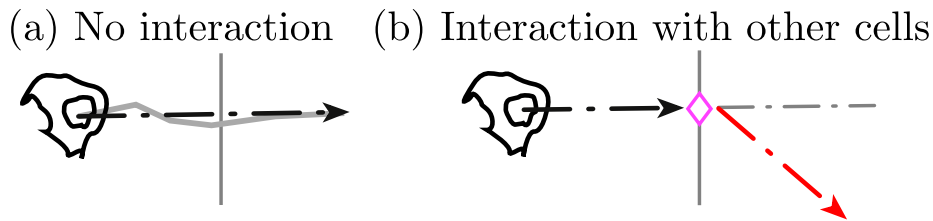## (a) No interaction   (b) Interaction with other cells

Fig. 1: Outline of the main hypothesis in this work. The interactions of the cells in a clump appear to influence on the migration patterns of the cells. The diagram shows (a) the case where a cell's trajectory does not change significantly from a point chosen arbitrarily; (b) shows the expectation of a cell that interacting in a *clump* and changing direction noticeably.

2   MATERIALS

Three different experiments of fluorescently labelled macrophages of the model organism *Drosophila melanogaster* were observed, producing three distinct videos of migrating macrophages. In each of the experiments, the nuclei were labelled with GFP-Moesin, appearing red, while the microtubules of the cells were labelled with Clip-GFP, a microtubule probe that appears green [5]. The three datasets contain RGB images of size $(n_w, n_h, n_d) = (512, 672, 3)$ at a pixel density of $0.21 \mu m$/pixel and two layers of fluorescence. The number of frames per dataset is 541, 361 and 462 frames, respectively. In a previous development [11], overlapping cells were studied and how to separate them. Overlapping cells were referred to as *clumps* and will be considered points of interaction between cells. Figure 2 contains an example frame and detail of the clumps, where interactions between cells can be appreciated.
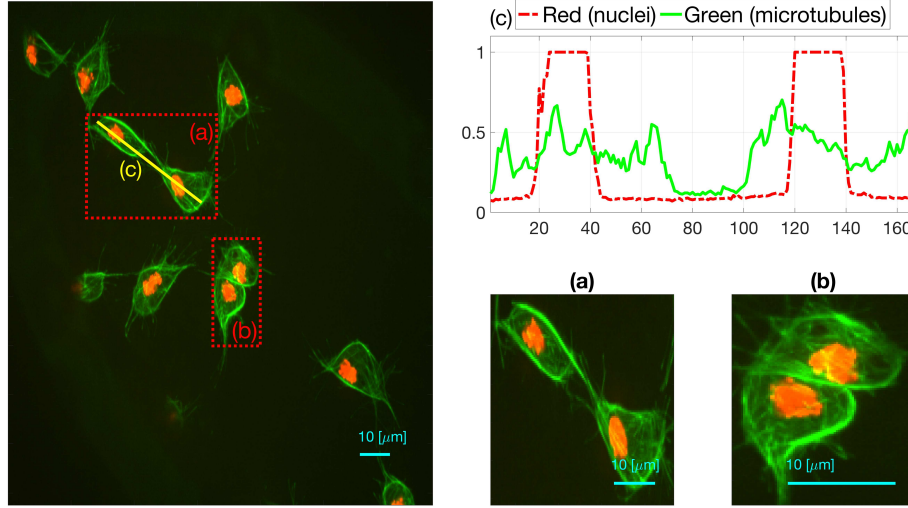
Fig. 2: Representative time frame highlighting in red (a,b) the interactions between cells. (c) Shows the intensities for the red and green channel along an image profile (yellow, solid). Detail of the highlighted pairs of cells, (a) and (b) are shown. Bars $10\mu m$.

The *clumps* in this work will be studied as points of potential interactions between two or more cells. Empirical observation of the data suggest that the interaction of the cells, which cause *clumps* could influence the migration pattern of the cells involved. Figure 3 displays a series of frames taken from a couple of cells that overlap and then appear to change direction.

3   METHODS

The method in this work can be divided into four stages of analysis. First, the segmentation of each channel individually. Then, the tracking of the objects detected in the red channel is performed, and the detections of each channel are classified as clumps or single cells. Finally, for each track, the change of direction (Δ Direction) is found before and after a given clump. Figure 4 shows a graphical representation of the procedures carried out in this work. Each stage is detailed in the following sections.

3.1   Segmentation of fluorescence intensity channels

The segmentation procedure for segmenting each of the respective channels follows three steps, fully described in [11]. Following a low-pass filtering, each channel was segmented by a hysteresis thresholding technique [12]. Finally, a morphological opening with a disk structural element ($r = 3$) was performed to remove noise and smooth the edges. Detection of clumps was achieved by comparing the number of nuclei detected within the area covered by each segmentation of the green channel.
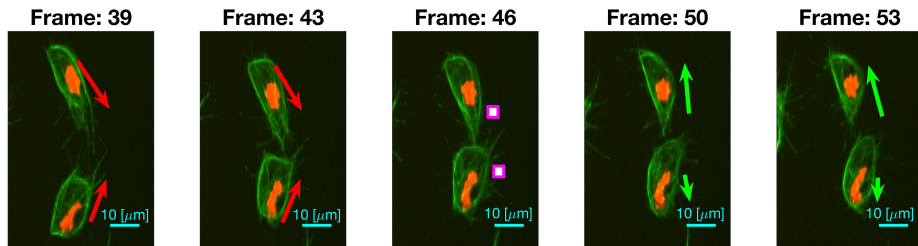
Fig. 3: Representation of the movement of two cells before and after the interaction (*clump*). Five frames are shown with arrows which represent the observed direction of movement, before (red) and after (green) the clump. **Frame 46**, in the centre, shows an interaction between the two moving cells, where a clump would be formed. Bars $10\mu m$.
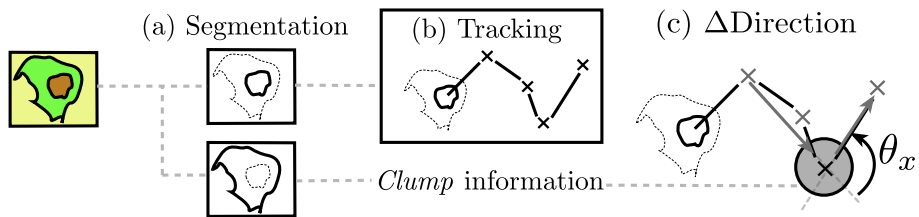

Fig. 4: Graphical illustration of the analysis done in this work. Three principal phases are depicted. (a) Segmentation of each fluorescence channel. (b) Tracking of the red channel and identification of each clump. Each mark ($\times$) in the diagram corresponds to a different time frame. (c) Finally, the measuring of the change of direction angle (θ_x) before and after a detected clump.

3.2 Tracking of the nuclei using PhagoSight

Tracking, defined in this work as linking the segmented objects in the RED channel, was performed through the PhagoSight software [12,13] a framework for cell tracking that uses the Keyhole algorithm [14,15].

The Keyhole Tracking Algorithm. The algorithm is a technique that links the segmented objects in contiguous frames through the analysis of the velocity and direction of the object at frames $t-1$ and t and estimating the position of the object at frame $t+1$. The methodology assumes that the most likely position of the child object, that is the one at $t+1$, will follow on the same direction and velocity of the object at present frame, t, and parent, object at $t-1$. As changes in the velocity and direction are possible, the algorithm generates two regions of probability set to anticipate for the child object's landing in frame $t+1$. The name of the algorithm follows the shape of the probability regions defined, which together resemble an old style keyhole. The distance between the parent and present objects, l, is used to define two regions: the *wedge*, which is an arc of length $\theta_w = \pi/3$ and radius $r_w = 3 \times l$ to accommodate for objects accelerating; and the *circle*, which accounts for the rest of the $\theta_c = 5\pi/3$ arc not covered by the wedge, and that has a radius of $r_c = l/2$. Figure 5 shows the different regions defined previously.
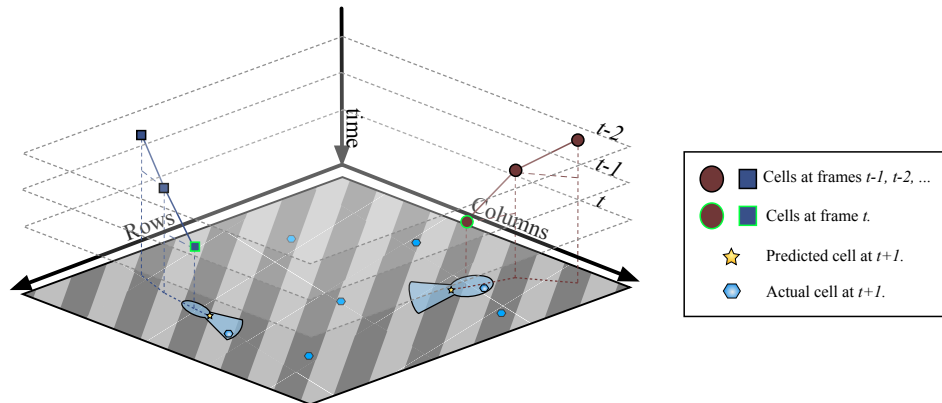

Fig. 5: Graphical illustration of the Keyhole algorithm. Two examples of different velocities are shown. A landing position is predicted taking into account the velocity of the previous frame.

Addition of clump information. Each track produced by PhagoSight includes the information of the cell's nuclei that has been tracked and linked from one frame to others. The information of interest to this work is explained in Table 1, it includes parameters such as time frame, position and velocity of each nuclei at each time frame. At each point in time, the presence of clumps was detected by counting the number of nuclei contained within a single object detected in the green channel.

As each nuclei within a clump has a track associated to them, each clump can be uniquely identified via a simple *unique identifier number* or for short *code*, which includes the labels of the tracks conatined within it. For instance, let r, q be the labels of two tracks ($r < q$) which at a certain point in time belong to a *clump*, then the code c is defined by $c(r, q) = c(q, r) = 1000q + r$. The value of 1000 is chosen arbitrarily as a large number, larger than the number of total tracks. Notice how the tracks' labels are arranged from left to right starting with the highest identifier to the lowest; for example, code 24013 would correspond to a clump that at a certain frame contains tracks 24 and 13. The previous definition can be extended for an arbitrary number of labels m interacting in the same clump as $c(r_1, \cdots, r_i, \cdots, r_m) = \sum_{i=1}^{m} 1000^{i-1} r_i$.

Table 1: Brief description of the parameters measured per track.

Field	Description
Time frame	Frame in the dataset where the following parameters were measured.
Position (x_t, y_t)	Cartesian coordinates of the centroid of the detected nucleus.
Velocity	Calculated with the position of the previous frame.
Track label	Unique identifier for each track.

Each clump can be uniquely identified based on the tracks contained in it. Table 2 shows a simple example of the creation of the clump codes. The inclusion of the codes facilitates the analysis of the cells that interact with each other.

Table 2: Examples of clump codes created through the track labels obtained by PhagoSight by applying the defined codes. See text for detailed explanation.

Clump code	Code construction $c(\cdot)$	Tracks within *clump*
2001	$c(2, 1) = 2000 + 1$	2,1
3002	$c(3, 2) = 3000 + 2$	3,2
5003002	$c(5, 3, 2) = 5000000 + 2000 + 1$	5,3,2

3.3   Measuring the change of direction before and after a clump

The algorithm developed in this work, estimates the angle formed between the direction of the cell prior to an interaction (*clump*) and the direction of the cell once the interaction is over and it does not belong to any clump. Let $\theta_x \in (-\pi, \pi)$ be the angle that measures the direction change (Δ direction). Let a track with label r, given by $T_r = \{(x_t, y_t) \in \mathbb{R}^2 | t = t_1, \cdots, t_T\}$, interact with another T_q through a *clump* with code $c(r, q)$, such that the overlap between the two cells happens at time frames $t_{k_0}, t_{k_1}, \cdots, t_{k_C}$. The determination of θ_x involves analysing the tracks T_r, T_q starting S frames before t_{k_0} and finalising at S frames after t_{k_C}. Frames $t_{k_0-S}, \cdots, t_{k_C+S}$ will be referred to as the *clump span*;

likewise, the time frames where the tracks are interacting, $t_{k_0}, t_{k_1}, \cdots, t_{k_C}$, will be referred to as *clump length*. Figure 6 shows a schematic of the tracks analysed and the choice of the time frames. Figure 9 displays the process of selecting the lines from which direction before and after the clump will be selected, and the way the angle will be measured. The estimation assesses the change of direction of each cell that exits a *clump*, relative to the orientation it has entering it.
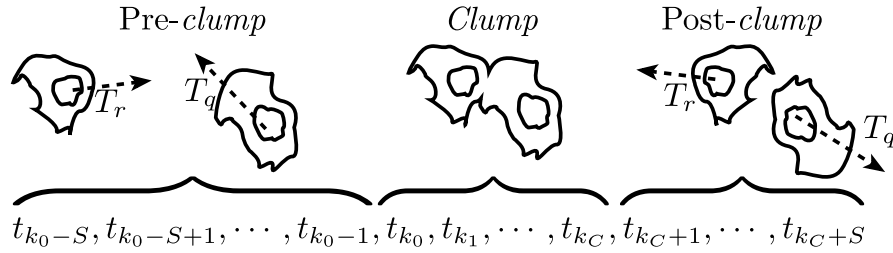

Fig. 6: Diagram explaining the time frames chosen from tracks T_r, T_q for the analysis of direction change. The time frames chosen for the analysis are S frames before t_{k_0} and S frames after t_{k_C}. The time frames are selected, and schematics of the cells moving are shown for each stage.

3.4   Experiments

All three datasets were segmented in both and tracked. The tracks' information was searched to find cases of clumps that fulfil the following criteria:

1. **Only two cells interacting.** There are cases where more than one cells integrate a clump. These cases were excluded from the analysis as it is not clear whether the interaction of more than two cells would be different from the interaction between a pair.
2. **In and out cases.** The cases selected only involved cells with a well-defined *clump span*, in which the cell would enter the clump and exit it without disappearing or interacting with other clumps.
3. **Immediate reaction.** A small value for $S = 5$ was chosen to define the *clump span*, as the interest of this paper is to study the immediate reaction of a cell after interacting within a clump. In this work, the *clump length* was not taken into consideration.
4. **Both cells in clump.** Cases where both tracks in the clump had a well-defined *clump span* were preferred as they would allow an analysis per *clump*.

Once the tracks were selected, the θ_x angles were calculated for each case. Additionally, for each track selected, the $2S$ time frames leading up to the *clump* were selected to compare the change of direction with a cell that has not interacted with a clump.
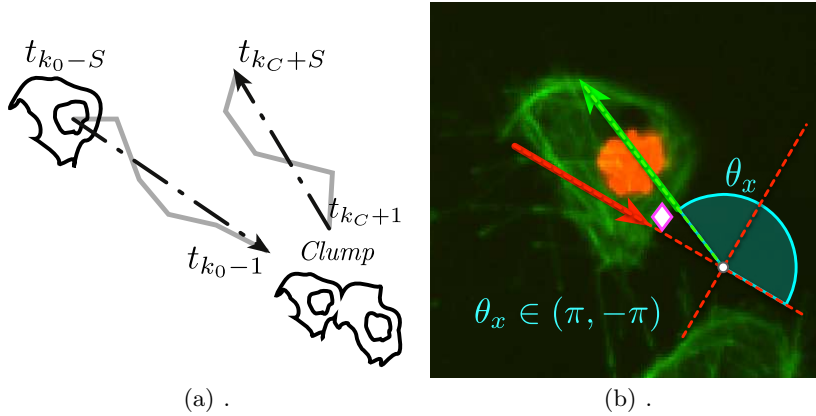
(a) .   (b) .

Fig. 7: Diagram explaining the calculation of the angle of direction change (θ_x). (a) Shows the determination of the direction before and after the clump, while (b) displays the calculation of the angle θ_x from the previously selected lines. The red arrow represents the line generated by points at times t_{k_0-S} and t_{k_0-1}, while the green arrow shows the points at times t_{k_C+1} and t_{k_C+S}.

4   RESULTS

All datasets were segmented and tracked, however, only two datasets were considered for the change of direction analysis due to inconsistent tracks being present, where a single cell would produce more than one tracks. Based the criteria in Section 3.4, thirty eight cases between the two datasets were selected.

Figure 8 displays an example of two cells interacting through a given *span* and the orientation lines before (red) and after the *clump* (green). To showcase the calculation of their respective θ_x, Figure 9 is included to show the *clump span* of (a) and (b), reoriented and displaying the arc of θ_x in magenta. Finally, all the 20 tracks selected for one dataset are shown in Figure 10, trying to show qualitatively the hypothesis depicted in Section 3.4, Figure 1. The angles of direction change θ_x in the experiments with interactions (a) had a mean of $37.4° \pm 77.65$ while the mean of the angles of the cells that do not interact (b) was $1.01° \pm 82.2$. The Wilcoxon Signed Rank test [16] was implemented to compare the results, and with a $p > 0.05$ the null hypothesis could not be rejected.

5   DISCUSSION

Preliminary work in this field [11] did not consider the inclusion the images analysed in the temporal context; only focusing in disambiguating the lost information of overlapping regions in the *clump*. In this work, a different approach to the analysis of migrating macrophages is presented. Its main contribution is to provide a framework for the analysis of movement of macrophages overcoming the difficulties of the challenging green channel.
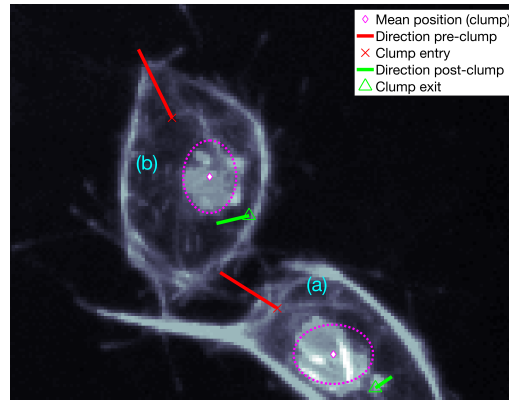
Fig. 8: Change of direction before and after a clump. A frame which contains both interacting cells, (a) and (b), is shown. The lines and points marked represent a collection of frames before and after the cells interacted in a *clump*. The mean position of each nuclei while in the clump is shown in magenta (⋄) and a dotted ellipse represents one standard deviation from the mean. Each cell presents a red solid line that shows the orientation of movement before the clump, and a green line that represents the orientation of movement after. Figure 9 shows a simplified view of the same cells' changes in orientation.
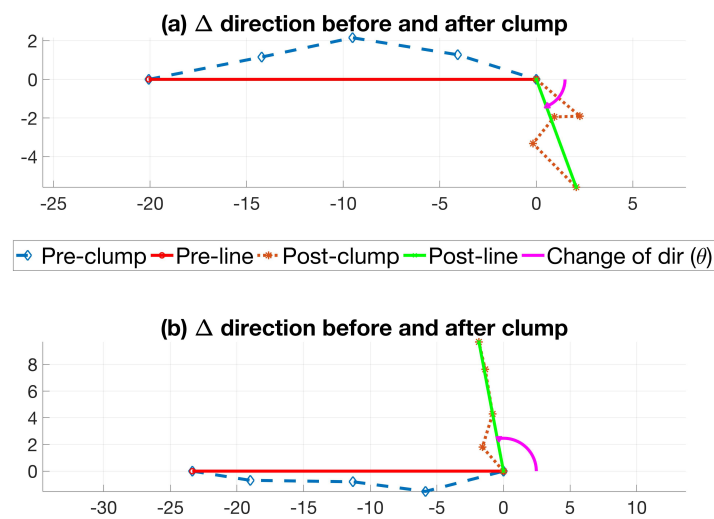

Fig. 9: Representation of change of direction before and after a clump. The tracks of the cells depicted in Figure 8 are shown. (a) and (b) represent a single cell's trajectory before and after interacting in a *clump*. The red lines represent the trajectory before the clump and are formed by the first and last points in the cells path (blue $-\diamond-$). The green lines show the orientation after the interaction. Each green line has been rotated in proportion to the rotation of the respective red line. The path of the cell after the clump is shown in orange (: ∗).
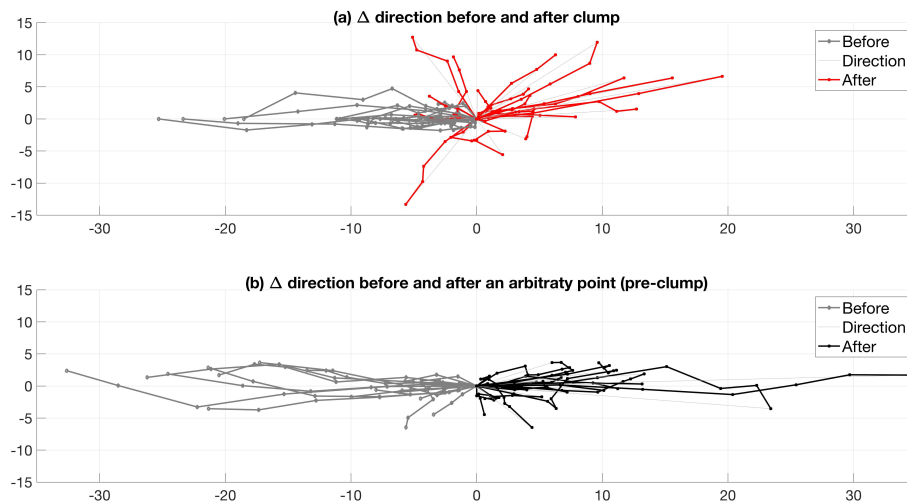
Fig. 10: Comparison of the changes in track directions with or without clump interaction within the entire dataset ($N = 20$). The sold line represents a cell's trajectory and the markers ($\cdot$) represents the position at a certain time frame. Each line can be read from the utmost left point and continuing along the line to the next time frame marker. (a) illustrates cells entering or exiting a clump, where the origin (0,0) represents the clump formation. Grey lines represent 5 time frame points of each cell's track before entering a clump. Red lines represent 5 time frame points of each cell's track after exiting a clump. (b) illustrates the movement of cells before entering a clump, where the origin (0,0) represents a chosen arbitrary point (time frame 6). This experiment is the realisation of the experiment proposed in Figure 1.

The algorithm also provides early insights into the relationship between the interactions between cells and the movement patterns, as shown by Figure 10, where the cells involved in an interaction (a) show much more variability and it appears, wider angles compared to the cells that do not interact (b).

The limitations of the algorithm involved the underlying limitations of the segmentation and tracking methods at dealing with complicated interactions. First of all, one of the datasets was excluded from the analysis as the tracks were inconsistent upon manual verification. The problems could be inherited from the limitations of the keyhole algorithm, which only considers velocity and previous direction to estimate the upcoming position. The problems could also be due to segmentation, as the dataset in question, contains more variability in the intensities than the ones used in the analysis, as well as a larger number of cells interacting in each clump. Future work could improve this by incorporating post-processing to the tracks.

Referring to Figure 10 the difference between the means of the angles could not be proven significantly different. This fact could have various explanations, which will be addressed in future developments of this work: (i) A deeper understanding is needed in terms of the value of S, for the amount of frames to be taken before and after the start and end of the clump; (ii) the *length of the clump* was not taken into consideration, and sometimes larger *clumps* could introduce other variables not accounted for, or interactions not quantified (Figures 8 and 9); finally, (iii) the calculation of the direction was done simply by taking two points before and after the clump, future work will include more sophisticated models of to assess an overall direction considering some or all the points.

It is worth noting that the movement that is being tracked in this work involves only the nuclei in the red channel. A more complete analysis could the shapes of the cells in the green channel as they evolve through time, as introduced in [17]. Such an analysis, incorporated into the idea presented in this work could lead to more precise insights about the movement of macrophages in time, and a better understanding of the moving patterns of the cells upomn interaction.

References

1. Martinez, F.O., Sica, A., Mantovani, A., Locati, M.: Macrophage activation and polarization. Frontiers in Bioscience: A Journal and Virtual Library 13, 453–461 (Jan 2008)
2. Wood, W., Martin, P.: Macrophage Functions in Tissue Patterning and Disease: New Insights from the Fly. Developmental Cell 40(3), 221–233 (Feb 2017)
3. Chawla, A., Pollard, J.W., Wynn, T.A.: Macrophage biology in development, homeostasis and disease. Nature 496(7446), 445 (Apr 2013)
4. Pocha, S.M., Montell, D.J.: Cellular and molecular mechanisms of single and collective cell migrations in Drosophila: themes and variations. Annual Review of Genetics 48, 295–318 (2014)
5. Stramer, B., Moreira, S., Millard, T., Evans, I., Huang, C.Y., Sabet, O., Milner, M., Dunn, G., Martin, P., Wood, W.: Clasp-mediated microtubule bundling regulates persistent motility and contact repulsion in Drosophila macrophages in vivo. Journal of Cell Biology 189(4), 681–689 (May 2010)

6. Ulman, V., Maška, M., Magnusson, K.E.G., Ronneberger, O., Haubold, C., Harder, N., Matula, P., Matula, P., Svoboda, D., Radojevic, M., Smal, I., Rohr, K., Jaldén, J., Blau, H.M., Dzyubachyk, O., Lelieveldt, B., Xiao, P., Li, Y., Cho, S.Y., Dufour, A.C., Olivo-Marin, J.C., Reyes-Aldasoro, C.C., Solis-Lemus, J.A., Bensch, R., Brox, T., Stegmaier, J., Mikut, R., Wolf, S., Hamprecht, F.A., Esteves, T., Quelhas, P., Demirel, , Malmström, L., Jug, F., Tomancak, P., Meijering, E., Muñoz-Barrutia, A., Kozubek, M., Ortiz-de Solorzano, C.: An objective comparison of cell-tracking algorithms. Nature Methods (Oct 2017)

7. Maška, M., Ulman, V., Svoboda, D., Matula, P., Matula, P., Ederra, C., Urbiola, A., España, T., Venkatesan, S., Balak, D.M.W., Karas, P., Bolcková, T., Streitová, M., Carthel, C., Coraluppi, S., Harder, N., Rohr, K., Magnusson, K.E.G., Jaldén, J., Blau, H.M., Dzyubachyk, O., Křížek, P., Hagen, G.M., Pastor-Escuredo, D., Jimenez-Carretero, D., Ledesma-Carbayo, M.J., Muñoz-Barrutia, A., Meijering, E., Kozubek, M., Ortiz-de Solorzano, C.: A benchmark for comparison of cell tracking algorithms. Bioinformatics (Oxford, England) 30(11), 1609–1617 (Jun 2014)

8. Zimmer, C., Labruyere, E., Meas-Yedid, V., Guillen, N., Olivo-Marin, J.C.: Segmentation and tracking of migrating cells in videomicroscopy with parametric active contours: a tool for cell-based drug testing. IEEE Transactions on Medical Imaging 21(10), 1212–1221 (Oct 2002)

9. Hand, A., Sun, T., Barber, D., Hose, D., MacNeil, S.: Automated tracking of migrating cells in phase-contrast video microscopy sequences using image registration. Journal of Microscopy 234(1), 62–79 (2009)

10. Solis-Lemus, J.A., Huang, Y., Wlodkowic, D., Reyes-Aldasoro, C.C.: Microfluidic environment and tracking analysis for the observation of Artemia Franciscana. pp. 4.1–4.8. British Machine Vision Association (2015)

11. Solís-Lemus, J.A., Stramer, B., Slabaugh, G., Reyes-Aldasoro, C.C.: Segmentation and Shape Analysis of Macrophages Using Anglegram Analysis. Journal of Imaging 4(1), 2 (Dec 2017)

12. Henry, K.M., Pase, L., Ramos-Lopez, C.F., Lieschke, G.J., Renshaw, S.A., Reyes-Aldasoro, C.C.: PhagoSight: An Open-Source MATLAB® Package for the Analysis of Fluorescent Neutrophil and Macrophage Migration in a Zebrafish Model. PLOS ONE 8(8), e72636 (Aug 2013)

13. Kadirkamanathan, V., Anderson, S.R., Billings, S.A., Zhang, X., Holmes, G.R., Reyes-Aldasoro, C.C., Elks, P.M., Renshaw, S.A.: The Neutrophil's Eye-View: Inference and Visualisation of the Chemoattractant Field Driving Cell Chemotaxis In Vivo. PLOS ONE 7(4), e35182 (Apr 2012)

14. Reyes-Aldasoro, C.C.: Measuring the velocity of fluorescently labelled red blood cells with a keyhole tracking algorithm. Journal of Microscopy 229(1), 162–173 (2008)

15. Reyes-Aldasoro, C.C., Zhao, Y., Coca, D., Billings, S.A., Kadirkamanathan, V., Tozer, G.M., Renshaw, S.A.: Analysis of immune cell function using in vivo cell shape analysis and tracking. 4th IAPR International Conference on Pattern Recognition in Bioinformatics (May 2009)

16. Hollander, M., A. Wolfe, D., Chicken, E.: The One-Sample Location Problem, pp. 39–114. John Wiley Sons, Inc. (2015)

17. Solís-Lemus, J.A., Stramer, B., Slabaugh, G., Reyes-Aldasoro, C.C.: Shape analysis and tracking for migrating macrophages. In: 2018 IEEE 15th International Symposium on Biomedical Imaging (ISBI). pp. 1006–1009 (Apr 2018)